Cassegrain Solar Concentrator System for ISRU Material Processing

Anthony J. Colozza [1] *, Robert Macosko* [2]*, , Charles Castle* [3]
Qinetiq NA/NASA Glenn Research Center, Cleveland, Ohio, 44135

Kurt Sacksteder [4]
NASA Glenn Research Center, Cleveland, Ohio, 44135

Nantel H. Suzuki [5]
NASA Headquarters, Washington D.C,. 20546

and

James Mulherin [6]
Optical Mechanics Corp., Iowa City, Iowa, 52244

A 0.5 m diameter Cassegrain concentrator was constructed as a means of providing highly concentrated sunlight for the demonstration processing of lunar simulated regolith and other NASA In-Situ Resource Utilization Project (ISRU) reaction processes. The concentrator is constructed of aluminum with a concentration ratio of approximately 3000 to 1. The concentrator focuses solar energy into a movable tray located behind the concentrator. This tray can hold simulated regolith or any other material and or device to be tested with concentrated solar energy. The tray is movable in one axis. A 2-axis extended optical system was also designed and fabricated. The extended optical system is added to the back of the primary concentrator in place of the moveable test tray and associated apparatus. With this optical system the focused sunlight can be extended from the back of the primary concentrator toward the ground with the added advantage of moving the focal point axially and laterally relative to the ground. This allows holding the focal point at a fixed position on the ground as the primary concentrator tracks the sun. Also, by design, the focal point size was reduced via the extended optics by a factor of 2 and results in a concentration ratio for the system of approximately 6,000 to 1.The designs of both optical systems are discussed. The results from simulated regolith melting tests are presented as well as the operational experience of utilizing the Cassegrain concentrator system.

Nomenclature

A_e	=	primary mirror effective area
c_p	=	*copper specific heat*
dT	=	*change in copper calorimeter temperature*
dt	=	time step
I_{sf}	=	solar flux [W/m^2]
M_c	=	copper calorimeter mass
P	=	available power
V	=	calibrated solar cell voltage
η_p	=	primary mirror efficiency
η_s	=	secondary mirror efficiency

[1] Research Engineer, Mechanical Systems, 21000 Brookpark Rd MS 301-9, Cleveland, Ohio 44138
[2] Research Engineer, Mechanical Systems, 21000 Brookpark Rd MS 500-AOS, Cleveland, Ohio 44138
[3] Designer, Mechanical Systems, 21000 Brookpark Rd MS 500-AOS, Cleveland, Ohio 44138
[4] Chief RES Space Environment and Experiment Branch, 21000 Brookpark Rd MS 309-2, Cleveland, Ohio 44138
[5] Program Executive, Human Exploration and Operations Mission Directorate, 300 E-. Street, SW, Washington DC, 20546
[6] President Optical Mechanics, P.O. Box 2313, Iowa City, IA 52244

I. Background

Since identifying the makeup of the lunar soil (regolith) via the Apollo missions to the moon, NASA has been studying the processing of the regolith. In support of a lunar base the interest is in the production and storage of liquid oxygen on the moon. To produce oxygen from the lunar regolith requires heating the regolith to very high temperatures and in some processes heating the soil to the melt point. The hydrogen reduction process requires heating the regolith to just below the sintering temperature[1] whereas the carbothermal process requires the melting of the regolith.[2] Both of these processes have been successfully demonstrated showing the viability of producing Oxygen on the moon.[1,2]

In addition to oxygen production, the heating and or melting of lunar regolith is also of interest in the production of thermal wadis, engineered sources of stored thermal energy.[3] One application for the storage of thermal energy is in conjunction with a rover or other surface vehicle. In order to survive the 14 earth-day night period the rover systems must be kept warm. This takes a considerable amount of stored energy to provide heater power over this period of time. Another option would utilize a solar concentrator for heating the lunar regolith and parking the rover over the heated surface for the nighttime. The heated regolith would radiate heat to the rover maintaining its temperature.

Previous work has been performed on solar concentrator concepts and hardware development that can deliver direct solar energy to the processes under consideration. For oxygen production a solar concentrator concept was devised for use at the lunar South Pole, which takes advantage of the nearly continuous sunlight that occurs at the lunar South Pole.[4] In this concept solar energy is supplied to a hydrogen reduction reactor where the regolith is heated to temperatures just below the melt point. Hydrogen gas is flowed through the heated regolith where it reacts with oxides in the regolith producing water vapor and then liquid water. The hydrogen and oxygen are separated from the water via electrolysis and the oxygen is liquefied and stored. The hydrogen is recycled back through the reactor process. This same solar concentrator concept is adaptable to the carbothermal process.

In support of these concepts and other potential future interests in studying the process of melting lunar soil with direct solar energy, a Cassegrain concentrator system was designed, fabricated and tested. The results of this effort to date are discussed in this report.

II. Concentrator System Design

The proposed concept was to use a small concentrator to demonstrate the capability to melt lunar regolith stimulant. The concentrator size was limited to 0.5 m in diameter. From previous work in melting regolith stimulant in an open atmosphere it was estimated that on the order of 100 W/cm^2 is required to provide a melt at the concentrated sunlight location. This is a conservative estimate. There are indications that as low as 40 W/cm^2 would be sufficient however, a design to the 100 W/cm^2 value was chosen to provide some margin.[5]

The initial design for the concentrator consisted of a 0.5 m diameter parabolic mirror (area of 0.196 m^2) with a secondary concentrator at its focus. Sunlight falling on the primary mirror is reflected up and concentrated onto the secondary mirror. The secondary mirror reflects it back through the opening at the base if the primary mirror, to the focus of the mirror system, which is behind the primary mirror, as illustrated in Fig. 1. For initial testing the regolith is held in a container at the focus of the secondary mirror behind the primary mirror.

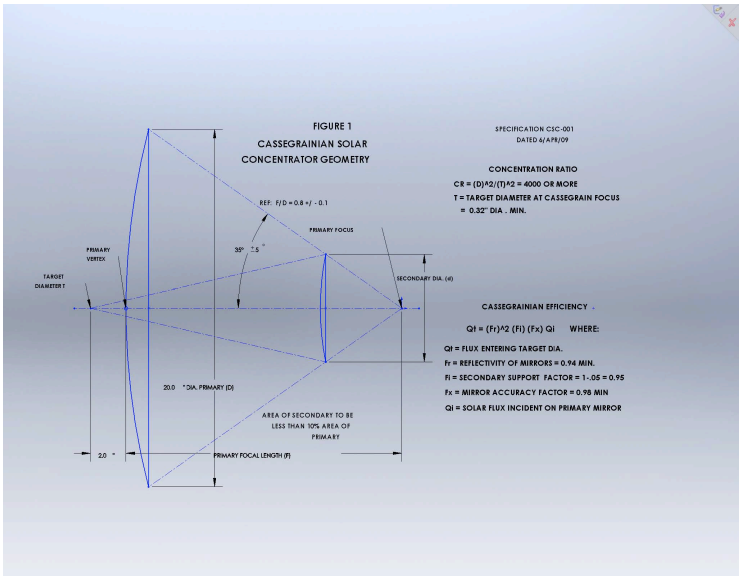

Figure 1. Detailed Concentrator Design Geometry.

Using this design and the size and concentration requirements the available power from the concentrator can be calculated. This available power is given by Eq. (1).

$$P = \eta_p \eta_s A_e I_{sf} \tag{1}$$

For this design it was assumed that the solar flux was 800 W/m^2. This is a typical value for a clear day near noon. However, on the lunar surface this value will be closer to 1400 W/m^2 throughout the day.

Shading of the incoming solar energy by the secondary concentrator and its support struts also has to be considered. The secondary mirror has a diameter of 0.15 m and there are 3 support struts holding the secondary mirror, which are 0.5 cm thick each. The three struts plus the secondary mirror have a shadow area of 0.021 m^2 onto the primary mirror. Accounting for this shadow area, the effective primary mirror area is 0.182 m^2. The losses due to the reflectivity of both the primary and secondary were then computed using silver coated aluminum surfaces with SiO protective coatings. With this surface finish, the efficiency of the primary) and secondary mirrors was conservatively estimated to be 0.9, as determined from Fig. 2. Over the wavelengths where most of the solar energy resides (.2 to 4 microns) the difference in reflectivity between aluminum and silver with protective coatings can be on the order of 5% (silver being the highest). To achieve the maximum power possible it was decided to utilize a silver reflective coating for both mirrors. The main concern with utilizing silver is its durability and lifetime. Degradation can occur quicker and easier than with aluminum ultimately requiring recoating.

Based on Eq. (1), the resulting power delivered to the focal point is 118 W. Therefore a spot size of 1.18 cm^2 is required at the mirror system focus for the desired power density of 100 W/cm^2. With a 0.52-degree sub-tense angle for the sun this spot size should be achievable with a reasonable focal length for the concentrator system. From the required spot size, the ratio of the primary mirror area to this spot area is 1661. This is the concentration ratio required by the mirror system. Both the determined spot size and concentration ratio are achievable with precision mirrors and the Cassegrain configuration.

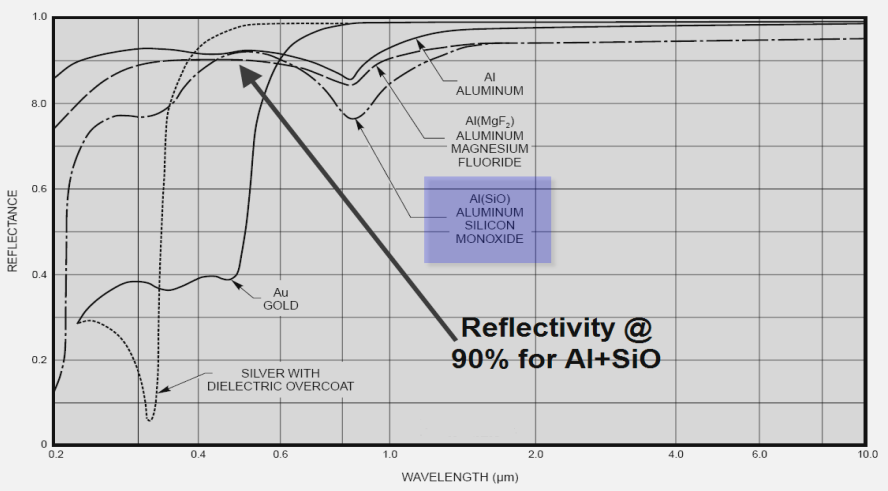

Figure 2. Sunlight Reflectivity of Silver and Aluminum

This initial evaluation indicated that the concentrator size and configuration was capable of being utilized to melt lunar regolith simulant and therefore a more detailed design was performed.

The primary and secondary mirrors were designed and constructed by Optical Mechanics Corporation. The design also included an adjustable holder for the secondary concentrator mirror with support struts and a mounting platform for attachment to a telescope-tracking mount.

In the design process, a detailed analysis using ZEMAX ray tracing software was performed on the mirrors to determine the mirror shape needed to position the focus a sufficient distance behind the primary mirror. A ray-trace of the primary and secondary mirrors is shown in Fig. 3.

Assuming perfectly shaped mirrors and very high specular reflective surfaces the spot size at the first focus was estimated to be 1 cm in diameter as shown by Fig. 4. Since perfect surfaces are never achieved the actual spot size achieved was expected to be slightly larger. The energy density within the spot is given by Fig. 5. The concentrator was designed so that the focus was located 2" (5.08 cm) behind the primary mirror.

The primary and secondary concentrators were fabricated from aluminum billets. The spherical primary concentrator was precision machined and polished. The elliptical secondary concentrator was diamond turned. Both concentrators were ion cleaned and then coated with vacuum deposited chrome, silver, and a protective silicon dioxide coating to achieve maximum reflectivity.

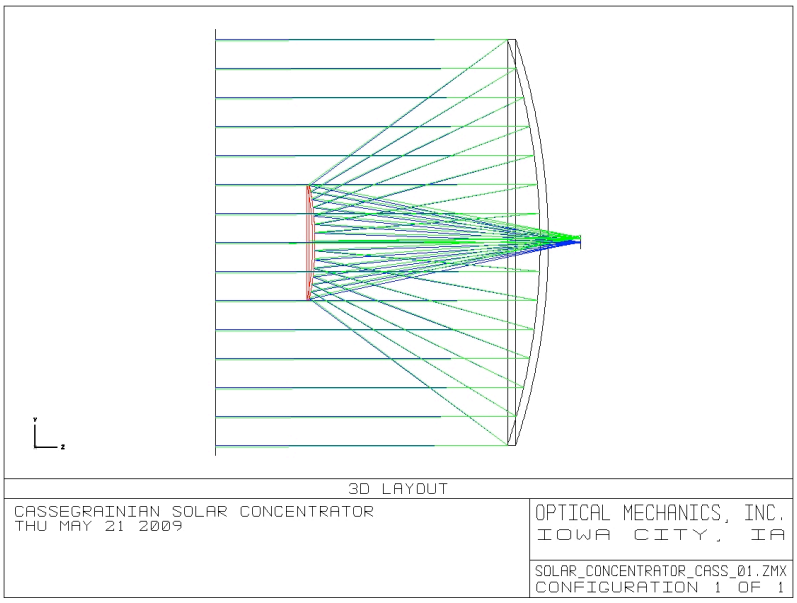

Figure 3. ZEMAX Ray-Trace

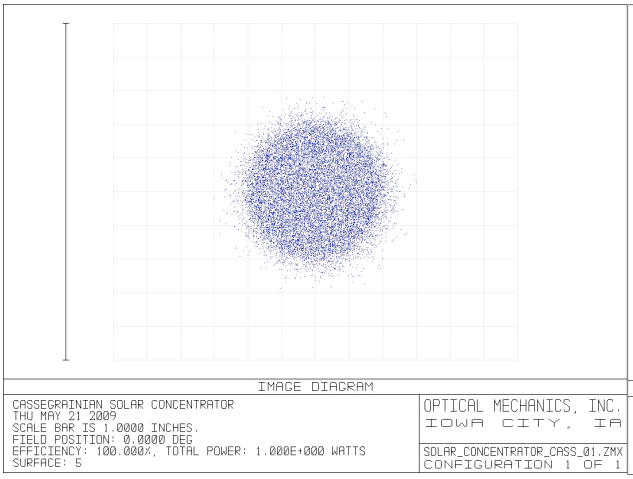

Figure 4. Ray Trace of Focus Spot

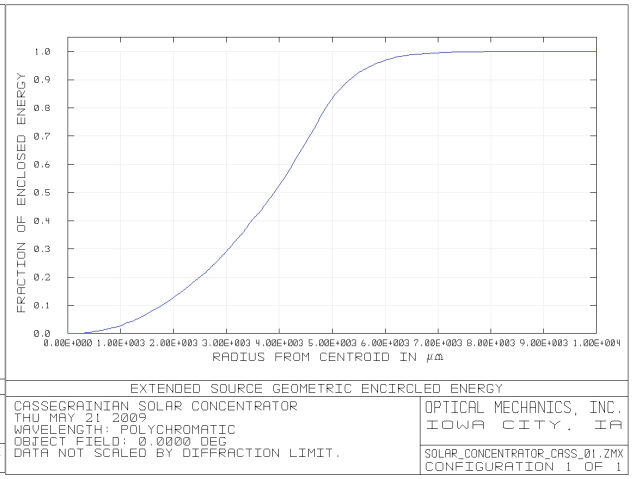

Figure 5. Focus Spot Energy Density

Based on this mirror sizing and layout the concentrator structure was designed. The structure positioned and held the primary and secondary mirrors as well as a tray for holding regolith simulant. This tray was located behind the primary mirror and was mounted on a rail, which allowed the tray to move in one axis perpendicular to the plane of the primary mirror. The rail and mounting supports for the tray positioned the top of the tray at the focus of the concentrator. The concentrator layout with the support structure and regolith tray is illustrated in Fig 6.

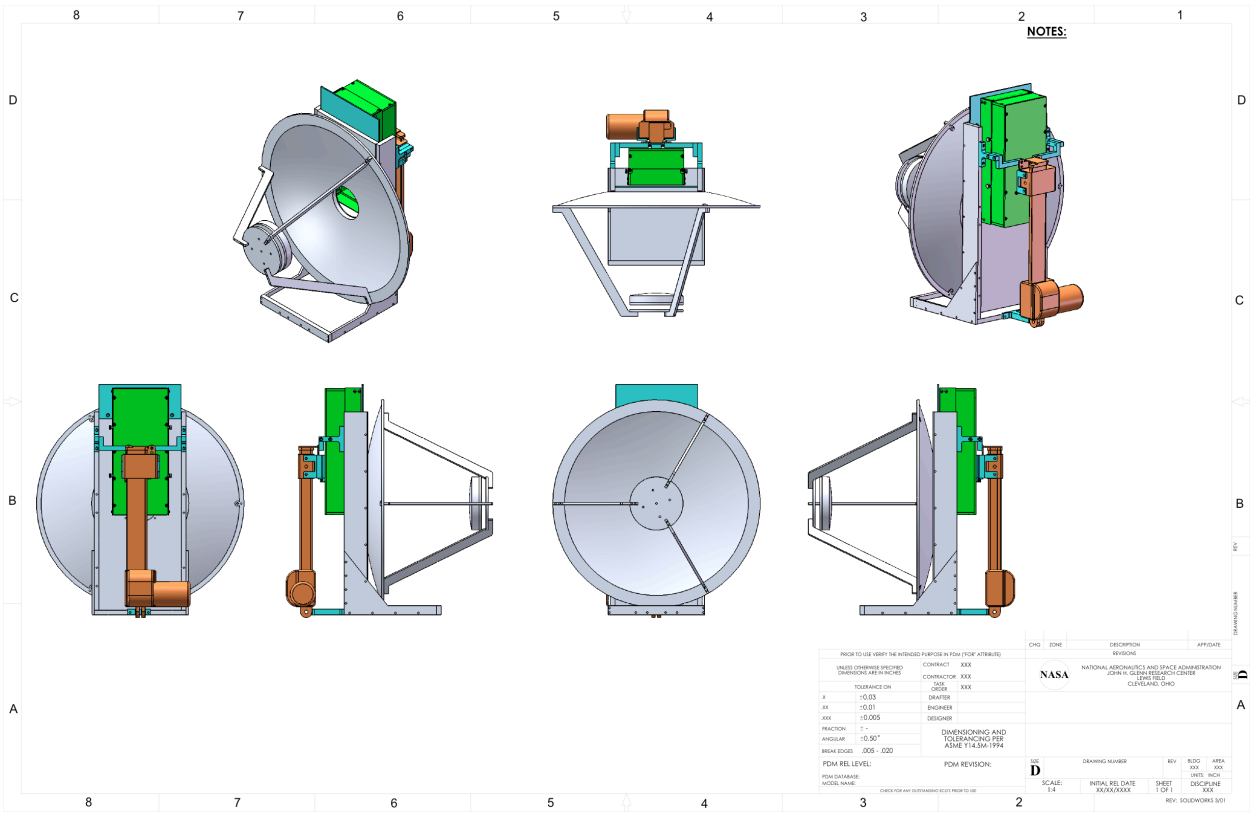

Figure 4. Concentrator Structural Design Layout

The concentrator was mounted on a Celestron CGE Pro equatorial, computerized, tracking mount. This type of mount was selected because it enabled the area behind the primary mirror, where the focus of the concentrator is, to be accessible. The concentrator, mount and tracker were placed on a metal trailer. The trailer provided a stable base and enabled easy movement of the concentrator system to and from outdoor testing. The trailer also had 4 screw jacks installed at the corners for leveling the platform. A bubble level was adhered to the mount to provide a leveling gauge.

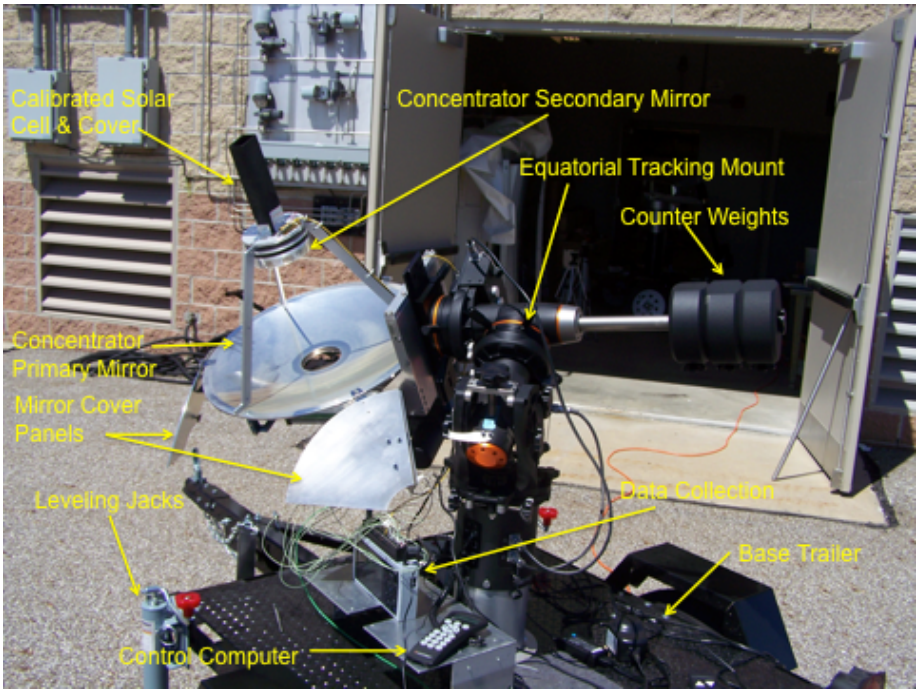

Figure 5. Cassagrain Concentrator System

A calibrated solar cell was mounted on the backside (sun facing) of the secondary mirror. This solar cell was used to determine the intensity of the incoming solar radiation falling onto the concentrator. To reduce the amount of diffuse radiation reaching the solar cell, a tube approximately 1 ft (~.3 m) in length was placed over the solar cell. The concentrator system is shown in Fig. 7.

III. Melt Testing of Simulated Lunar Regolith

A. Initial Melt Test

The first test goal was to achieve a successful melt of simulated lunar regolith. The first test was run on July 30th, 2010 at 10:35 am and was completed at 10:50 am.

This was approximately 6 months after the concentrator mirrors were coated. In this time the mirror coating had degraded limiting the amount of solar energy transferred to the regolith simulant. A successful melt however was achieved, with the mirror in the degraded condition. The regolith simulant, JSC-1A, was held in a styrofoam cup, placed in the regolith tray and centered at the focus of the concentrator, as shown in Fig. 8.

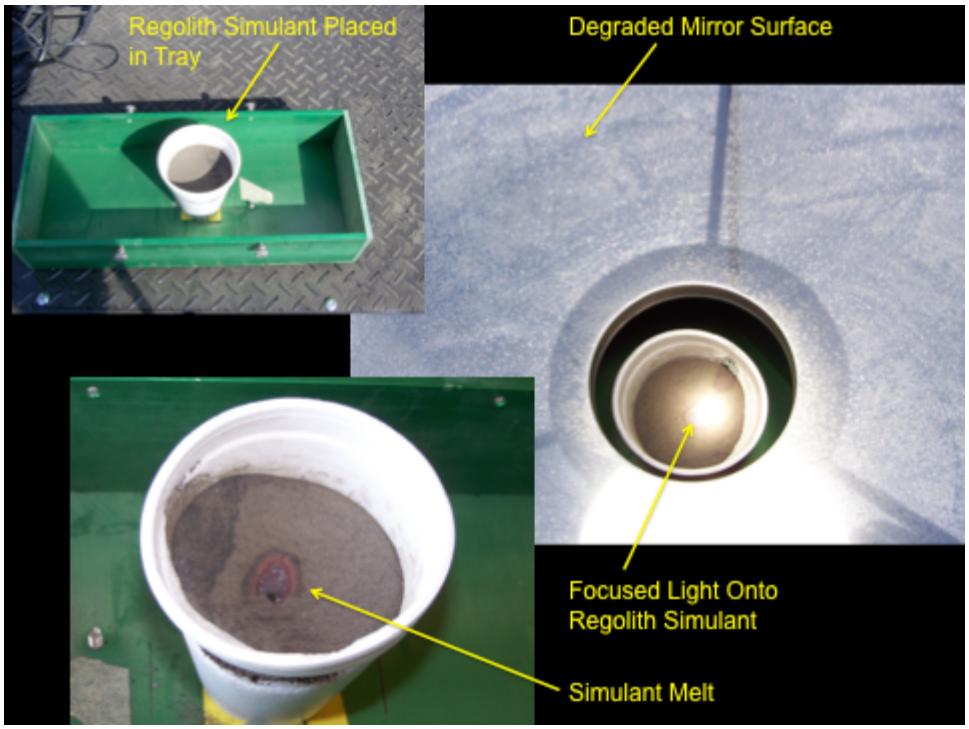

Figure 6. Initial Melt Test

The concentrator and tracking system worked fairly well. There was a slight drift of the focus over the operating period, which was due to a slight misalignment during the initiation of tracking. Accurately aligning the concentrator is somewhat difficult due to the configuration of the concentrator, lack of a spotting scope and the sun being the target focus. Various techniques were utilized throughout the tests performed with mixed results. For future tests a more reliable alignment system based on a spotting scope will be implemented.

For this testing the calibrated solar cell was not operational. To provide some gauge of the incoming power to the concentrator a hemispherical solar power meter was used to measure the solar flux. This meter measured both direct and diffuse solar radiation. This is not a completely accurate measure of the solar power available since the diffuse component is not usable by the concentrator. The total solar flux measurements are given in Table 1. Of the measurements taken it is estimated that between 200 to 300 W/m^2 was due to diffuse reflected light.

Table 1. Total Solar Flux During the Initial Melt Test

Time	Solar Flux (W/m^2)
10:40	**800**
10:45	**1134**
10:50	**1070**

The melt was removed and inspected to acquire its size. It measured 6.3 mm wide X 15.9 mm long X 1.5 mm thick. The power available at the focus to achieve the melt was not measured and the power density or distribution at the focus could not be determined. The above measurement is representative of the area of the spot at the focus where the energy density is sufficient to achieve a melt. During a longer test the melt is expected to grow deeper into the regolith as well as increase in diameter.

Since there was little sintering around the melt zone and there was a clearly defined boarder between the melted and un-melted region it can be concluded that the width of the melt zone is a good indicator of the very high quality of the optical surfaces of the concentrator. However, although the concentrator mirror's surface shape and precision are very high, the reflectivity was significantly reduced due to the coating failure.

B. Concentrator Efficiency Measurement

Following the successful initial melt test a calorimeter was fabricated to measure the power available at the focus, as shown in Fig. 9. It consisted of a copper heat receiver, 5 cm diameter by 7.6 cm length. The cylinder is high purity copper (99.999% copper) and has a 2.5 cm diameter hole drilled in it provided a 1.2 cm wall thickness. The hole extends to 1.2 cm from the bottom surface of the cylinder. This aperture is large enough to capture the entire solar beam at the focal point of the concentrator. The inside of the receiver was coated with a flat black paint to minimize reflection losses and the entire receiver was thermally insulated. The power absorbed by the heat receiver was determined using the specific heat of the copper material and the temperature rise of the copper heat receiver with time. The temperature rise was measured by eight type K thermocouples mounted on the heat receiver outer surfaces.

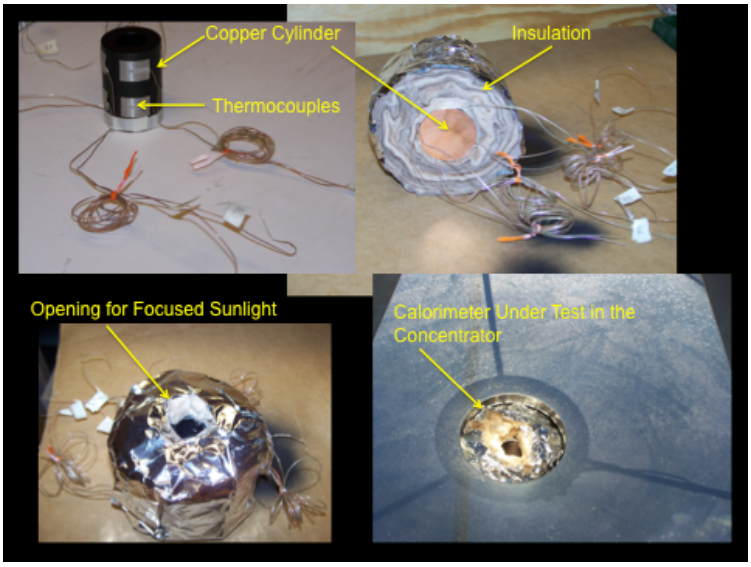

Figure 9. Calorimeter Construction & Use

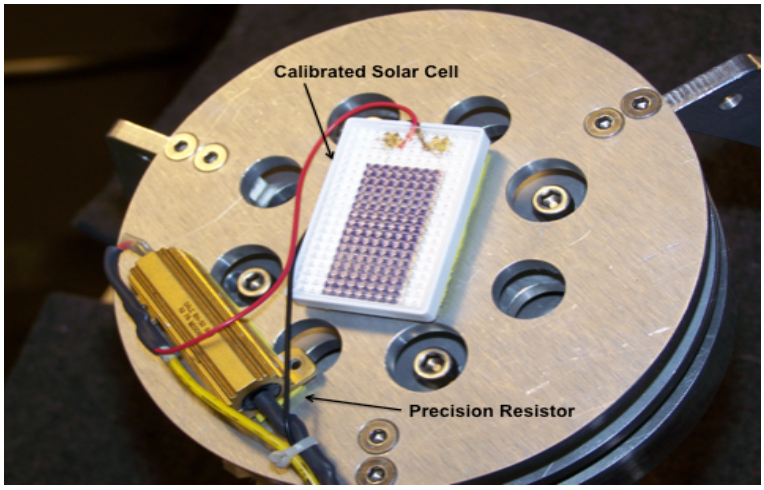

Figure 10. Installed Calibrated Solar Cell

Since the receiver temperature increases slowly and remains low the heat loss from the receiver due to radiation from the aperture is minimal.

The calorimeter was used in conjunction with the calibrated solar cell to determine the overall efficiency of the concentrator. The calibrated solar cell was installed on the backside of the secondary mirror, as shown in Fig. 10. The output of the solar cell was also used to help fine tune the position of the concentrator toward the sun prior to initializing the tracking.

The calibrated solar cell was connected to a precision 1ohm precision resistor to measure its output current. Since the resistor is 1 ohm there is a 1 to 1 correlation between the measured voltage and current produced by the solar cell. The solar cell current output is linear with the incoming solar radiation and was measured to produce 278 mA at 1000 W/m^2 incident solar radiation. From this the incident solar radiation (I_{sf}) can be determined from the measured voltage (V), as given by Eq. (2).

$$I_{sf} = 3.6V \tag{2}$$

The calorimeter tests to determine the concentrator efficiency were conducted at various times throughout the testing. These efficiency tests were repeated periodically because of the mirror finish degradation. These tests were used to establish the amount of power incident on the regolith during the melting tests. The efficiency tests were considered valid for a 2-week period. Outside of this period a new efficiency test would be run prior to performing a melt test.

The first concentrator efficiency test utilizing the calorimeter and calibrated solar cell took place at 10:45 am on September 1st 2010. The thermocouple temperatures and output of the solar cell were recorded and are show in Fig. 11.

The data began being collected at the beginning of the tracking setup for the concentrator. The heating of the calorimeter begins at about 180 s as can be seen by the sharp rise in the incoming solar power. The test portion of the graph runs from approximately 180 s to 410 s. The incoming solar power was constant through the test. This indicates that the conditions did not change during the testing and that the tracking system was aligned well and tracking the sun. The temperature of the calorimeter rose linearly throughout the test portion. This should be expected since the incoming solar radiation was constant over this time period. Also there was very little variation between the 8 thermocouples. This indicates that the sunlight was well distributed within the calorimeter and the calorimeter wall thickness was sufficient to effectively conduct the heat to provide uniform heating.

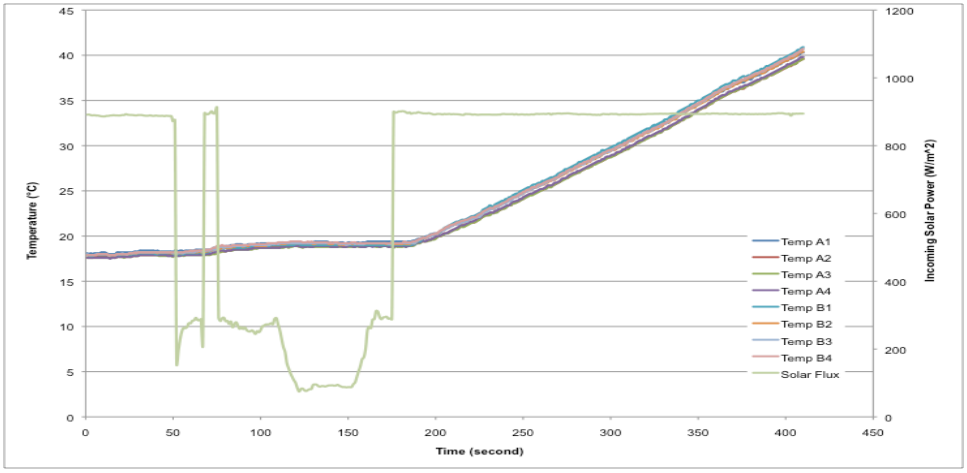

Figure 11. Calorimeter Test Thermocouple Temperature and Solar Flux

Using the temperature data collected the incoming power to the calorimeter was calculated from Eq. (3). The slope of the temperature curve for the calorimeter was 0.097 °C/s. The calorimeter is constructed of 99.999% pure copper, which has a specific heat capacity (c_p) of 384.9 J/kg°C and a mass of 1.1 kg.

$$P = M_c c_p \frac{dT}{dt} \tag{3}$$

From Eq. (3) the incoming power to the calorimeter was calculated to be 41 W. To determine the overall efficiency of the concentrator the power incident on the concentrator has to be determined. From the calibrated solar cell it was determined that the average incoming solar flux was 893.5 W/m^2. The area of concentrator main mirror is 0.2 m^2. Based on that area the incoming solar power was 181 W. Taking the ratio of the incoming solar power to the power entering the calorimeter the concentrator efficiency was calculated to be 23%. This fairly low efficiency is mainly due to the degradation of the coating and reflective surface of the primary and secondary mirrors. Also this efficiency does not take into account the area of the primary mirror shadowed by the secondary mirror and support struts. By subtracting these areas from that of the primary mirror the useable area and therefore power can be used to calculate the efficiency. The secondary concentrator and support struts have an area of 0.02 m^2, which reduces the power to the primary mirror to 165W. Based on the incident power value, the efficiency of the concentrator increases a few percent to 25%. It should be noted that the diffuse light shield was not utilized to shield the solar cell in this initial efficiency test. Since the diffuse light component cannot be utilized by the concentrator and therefore does not factor in to the power entering the calorimeter, eliminating the diffuse component would increase the calculated efficiency of the concentrator by a few percent. All subsequent efficiency tests utilized the diffuse light shield and therefore provided more accurate efficiency measurements.

C. Temperature Profile Melt Tests

To aid in the determination of power density needed to create a melt a thermocouple rake was fabricated that could measure temperatures at the surface and into the melt. The rake was used to provide temperature gradient and change measurements around the melt zone. The rake consists of 9 type-R thermocouples installed in 3 rows of 3 each as shown in Fig. 12. The rows are spaced 7 mm apart and within each row the thermocouples are spaced 5 mm apart. Thermocouples 1, 2 and 3 are located at the surface of the regolith. Thermocouples 4, 5 and 6 are in the middle row and 7, 8 and 9 are at the bottom row. The thermocouples are each supported with a ceramic sleeve. Styrofoam is placed around the area of the thermocouples to limit the amount of regolith in the tray, as shown in

Fig. 13. Due to the weight of the regolith, the less that is used the easier it is to balance the concentrator tracking system.

The cavity within the Styrofoam was filled with regolith. It was compacted during the filling process by slightly tapping on it and shaking and tapping on the tray. The regolith filled tray is shown in Fig. 13.

Once the tray was filled with regolith and the thermocouples connected to the data acquisition system, the tray was installed onto the concentrator. The regolith tray was adjusted so the center of the concentrator focus was centered at the tip of thermocouple 2, as shown in Fig. 14.

Typical simulated regolith melt regions are show in Fig. 15. This figure shows the melt zone for the regolith simulant as well as an area of sintered regolith simlant surrounding it. During these tests it was common for some of the surface simulant to be blown out of the tray by winds, as can be seen in Fig. 15.

Four rake melt tests were performed. After the first test the concentrator mirrors were sent back to the manufacturer for recoating. Once they were returned the concentrator was reassembled and placed in storage for the winter and early spring. The melting tests resumed in June. However, while in storage for 5 months, the coating began to degrade again. So the subsequent tests that took place during the summer months were also performed with degraded primary and secondary mirrors. The test conditions and results for these tests are summarized in Table 2 and the thermocouple temperature and incoming solar flux are plotted in Fig. 16 through Fig.19. The operating efficiency of the concentrator was determined from a calorimeter test performed prior (within 2 weeks) of the melt testing.

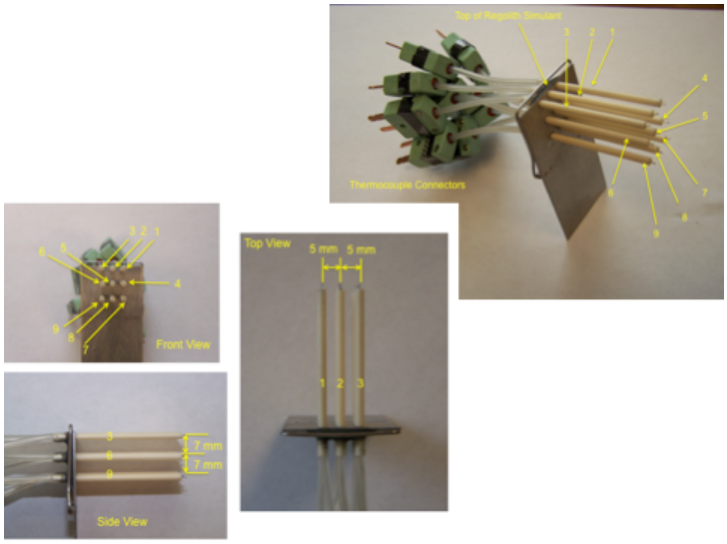

Figure 12. Thermocouple Rake

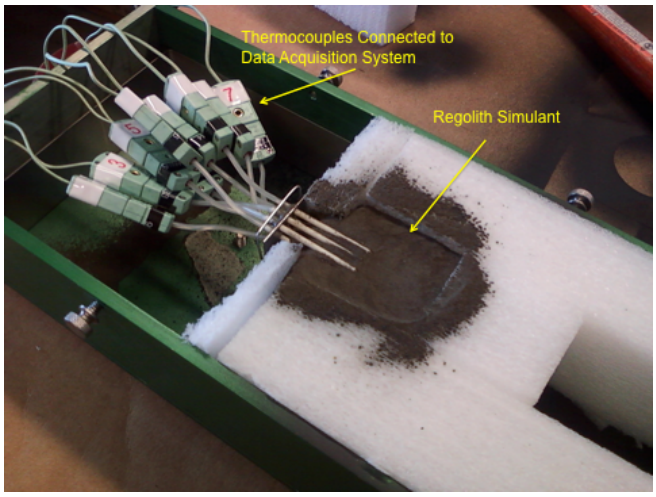

Figure 13. Thermocouple Rake Installed in Tray

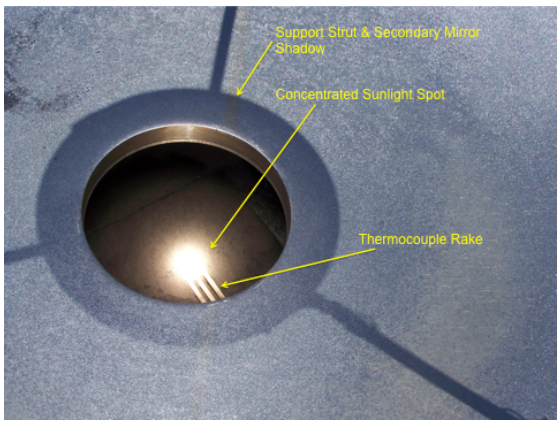

Figure 14. Melt Test Using Rake

The results from the first melt testing, held on September 24th, are plotted in Fig. 16. This figure shows the output temperature of each thermocouple and the incoming solar flux throughout the test. The test lasted just under 1½ hours. During this time the regolith tray position was adjusted twice, at approximately 300 seconds and 1600 seconds into the test. These slight adjustments were performed to better align the concentrator focus to the thermocouple position. These adjustments account for the increase in thermocouple temperatures seen at these times in the test data.

The maximum temperature was reached by thermocouple 1 at 880 °C. The focus was slightly off-set toward thermocouple 1. This accounts for the difference in temperature between thermocouple 1 and 3. At approximately 1700 seconds there was a drop-off in temperature and solar flux. The concentrator being shaded by a nearby communications tower caused this.

The tower was a truss structure and did not produce a noticeable shadow. However, as shown by the solar flux output the drop in incoming solar power was significant. Also a slight rise in solar flux is noticeable throughout the test. This rise is due to the increasing solar elevation angle that occurred during the testing. The peak solar elevation angle will occur at solar noon (approximately 1:00 pm, due to daylight savings time), which was after the test was completed.

The condition of the mirrored surfaces (which were operating at less than 10% efficiency), significantly limited the maximum temperature that could be achieved, along with the wind. Although regolith melt temperature of around 1200°C was not achieved, sufficient heat was provided to sinter a portion of the regolith.

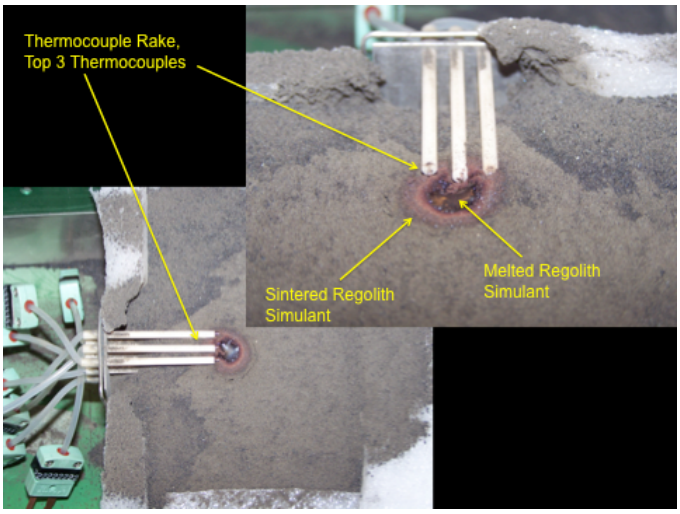

Figure 15. Thermocouple Rake Test Typical Melt Zone

Table 1 Operating Conditions for Melt Tests with Temperature Rake

Melt Test Run Date/Time	Conditions	Concentrator System Operating Efficiency (based on the total primary mirror area, 0.203 m^2)
September 24th 2010/10:36 AM	Clear day, no cloud cover with a little haze, windy with gusts of 20+ mph	8.0%
June 13th 2011/12:40 PM	Clear day, no clouds, calm little wind	36.5%
July 27th 2011/10.15 AM	Clear day with high cirrus clouds, calm little wind. Cloud cover increased during the testing.	23.8%
August 11th 2011/1:35 PM	Clear day with low humidity and no clod cover, moderate breeze (<10 mph)	23.8 %

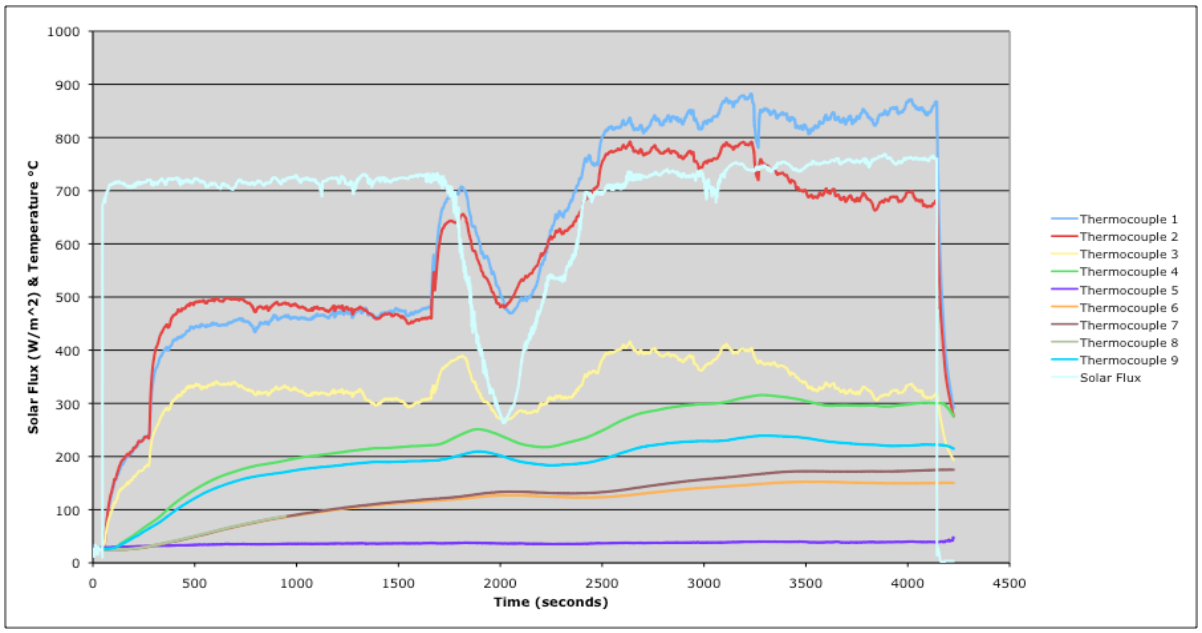

Figure 16 Rake Thermocouple Temperatures and Solar Flux for the 9-24-10 Melt Test

The second melt test utilizing the thermocouple rake was held on June 13th. The results from this test are plotted in Fig. 17. This figure shows the output temperature of each thermocouple and the incoming solar flux throughout the test. The test lasted just over 45 minutes. There was fairly good tracking alignments so no adjustments were done on the tray or concentrator during the test. The solar flux remained fairly constant throughout the test, increasing slightly due to the increase in solar elevation angle. The maximum temperature was reached by thermocouple 3 at 415 °C. The focus did drift during the test as can be seen by the drop-off in temperature of thermocouple 2. The thermocouples were not directly located at the focus and the focus was offset toward thermocouple 3. This caused a lower temperature reading of the thermocouples from the other tests. This is due to the low thermal conductivity of the simulant. The temperature of the simulant drops off significantly at small distances from the focus. Although the thermocouples indicated low regolith temperatures this was due to their positioning relative to the focus. The temperature at the focus was sufficient to produce a melt.

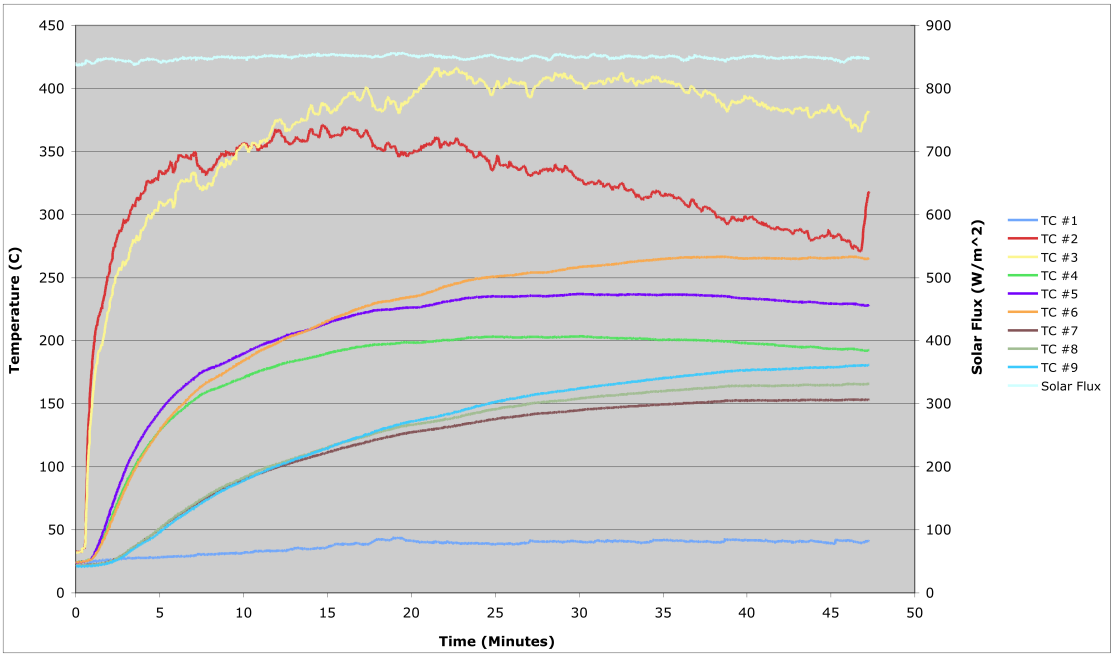

Figure 17 Rake Thermocouple Temperature and Solar Flux for the 6-13-11 Melt Test

The third melt test utilizing the thermocouple rake was held on July 27th. The results from this testing are plotted in Fig. 18. The test lasted approximately 35 minutes. The initial concentrator alignment was poor causing the focus to drift. The focus alignment was reset a number of times during the testing. This accounts for the sharp drop-off and rise in the temperatures of thermocouples 1, 2 and 3. The solar flux remained fairly constant throughout the beginning part of the test. After approximately 20 minutes the solar flux began to fluctuate due to high-level clouds obscuring the sun. This also caused a general decrease in the thermocouple temperatures. The test was stopped due to the increasing cloud cover. The maximum temperature was reached by thermocouple 3 at 925 °C.

A fourth and final regolith melt test utilizing the thermocouple rake was performed on August 11th. The test lasted approximately 45 minute. Due to the clear day and low humidity the solar flux was fairly constant throughout the test with a value above 800 W/m^2. The concentrated sunlight spot maintained its position throughout the test and no adjustments were necessary. Because the testing took place near solar noon, the concentrator and tray placement was nearly horizontal. This positioning had an added benefit in that it reduced the risk of the regolith moving or shifting during the testing. Even with the relatively poor condition of the concentrator mirror finish, a melt was successfully achieved. The central portion of the melt is located near the center thermocouple.

For this test, the melt zone was removed from the regolith tray and measured and weighed. It had a mass of 0.2 grams. Once the sintered material was removed the melt dimensions were approximately 9.5 mm long by 9.5 mm wide by 2.4 mm deep. This test provided the most uniform and consistent temperature data. Due to the good solar alignment with the concentrator, the temperature of all thermocouples increased uniformly throughout the test. The maximum temperature was achieved by thermocouple 2 at approximately 980 °C. The fluctuations in the surface

thermocouple temperatures (1, 2 and 3) were due to slight changes in the solar flux and winds slightly cooling the surface during operation.

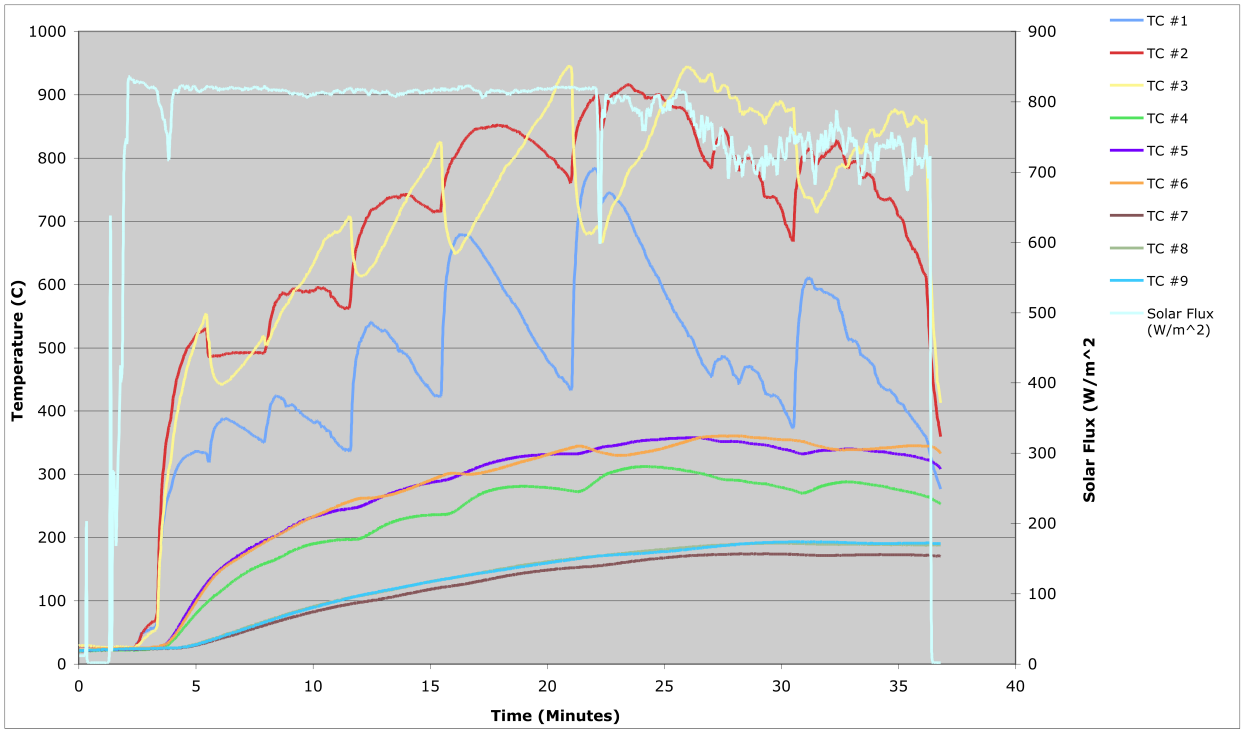

Figure 18 Rake Thermocouple Temperatures and Solar Flux for the 7-27-11 Melt Test

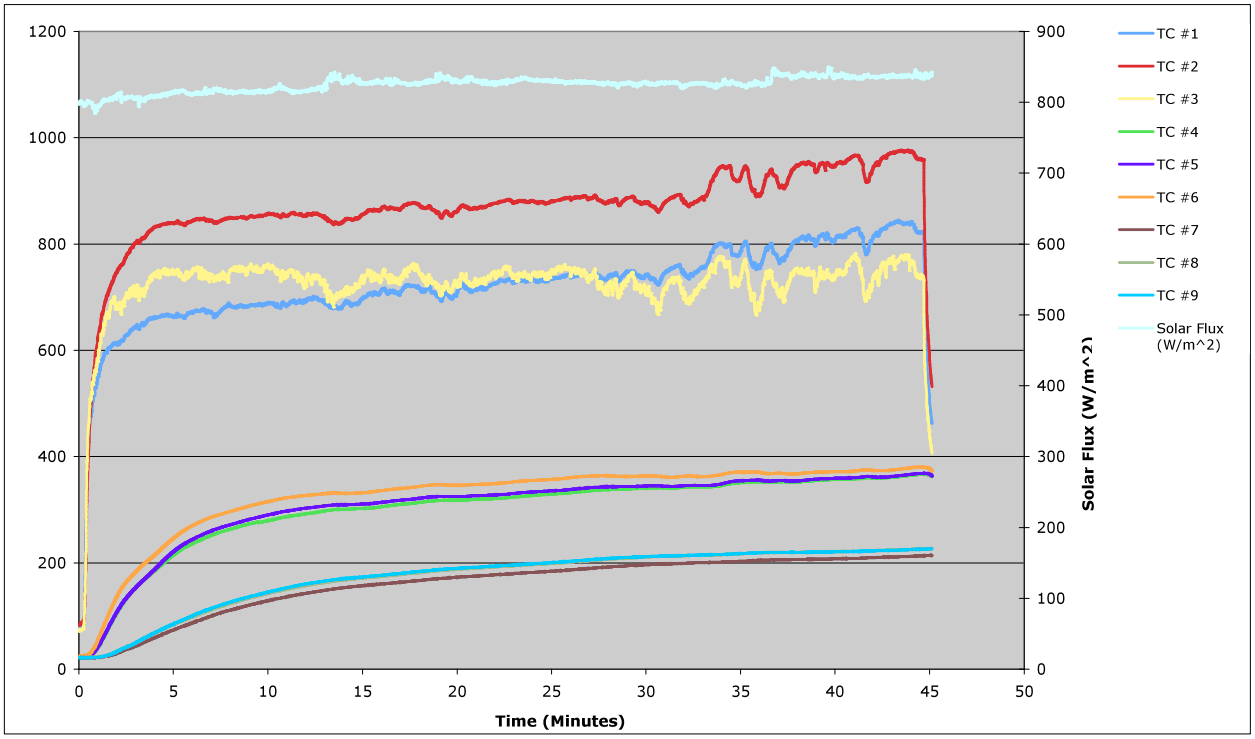

Figure 19 Rake Thermocouple Temperatures and Solar Flux for the 8-11-11 Melt Test

This final test provided a means of determining the actual energy density needed to start or produce a melt. The energy distribution at the focus is never perfectly uniform due to imperfections in the surface accuracy of the

concentrators and especially due to imperfections in the reflective surfaces of the concentrators. Visual inspection of the spot size relative to the known spacing of the rake thermocouples provided an estimate of the diameter of the spot. Using this dimension and assuming a Gaussian distribution of the power measured by the calorimeter test performed prior to this test yielded the Gaussian power distribution curve shown in Fig. 20.

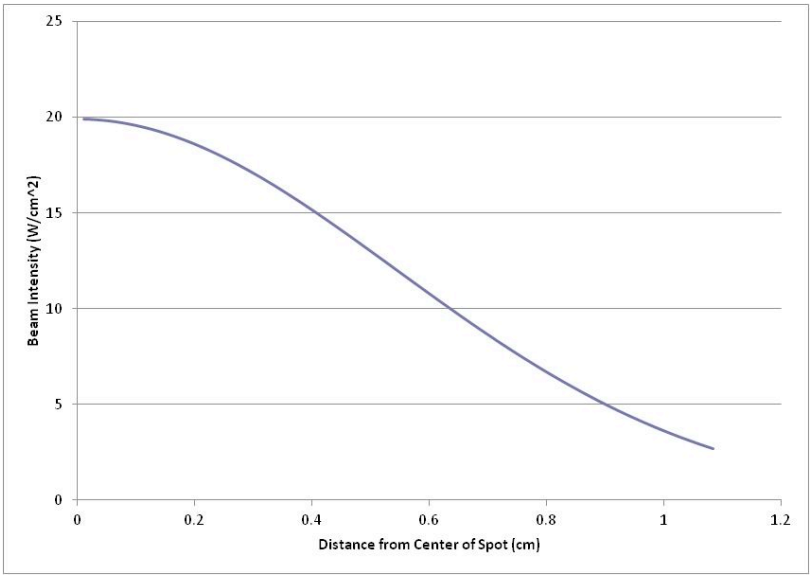

Figure 20. Gaussian Distribution of Solar Power at the Concentrator Focus

With the known dimension of the melt, the power density applied directly to the melt can be estimated. The spot size was visually estimated at 2.18 cm in diameter with an area of 3.63 cm^2. Based on the calorimeter test the power to the spot was 36.79 watts. The melt top area measured 0.95 cm in diameter corresponding to an area of 0.708 cm^2. Using a Gaussian distribution of the incoming power (36.79 watts) yields a peak value at the center of the melt of 20 watts/cm^2 and a value at the edge of the melt of 13 watts/cm^2. From this analysis it appears that a lower watt density than the 100 watts/cm^2 estimate derived from earlier ISRU testing is needed to start and grow a melt. Further testing is needed with the Cassegrain system at higher total power levels and shorter time periods to verify this result. Also an IR camera could be implemented for a better determination of the spot size at the focus and the temperature distribution within it.

IV. The Addition of Extended Optics

To improve the capabilities and performance of the Cassegrain concentrator an extended optics system was devised to provide enhanced concentration ratio as well as provide control of the location of the concentrator focus. This system would enable the concentrator to focus light to a spot on the surface and maintain focus onto that spot as the concentrator tracks the sun. The system provided both the means to adjust the location of the focus and the distance it was from the concentrator.

The design allowed for a total extension of the focal point to a distance of 23 inches (58.4 centimeters) from the back of the primary concentrator. The ray trace of the final design is shown in Fig. 21.

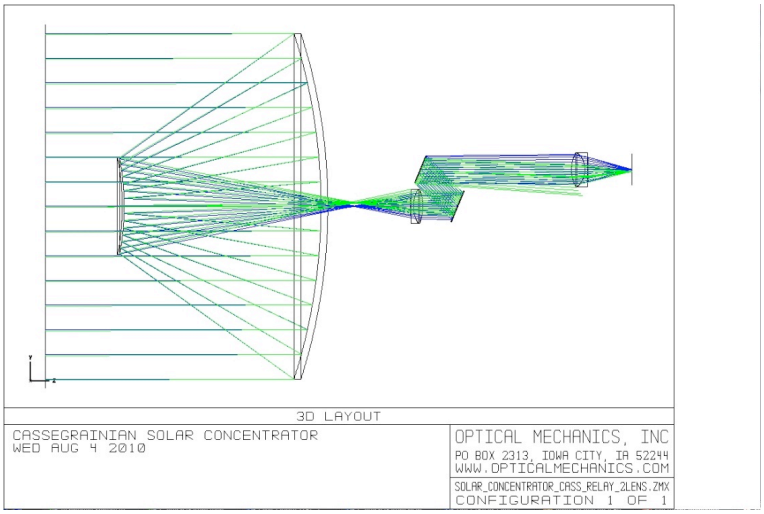

Figure 21. Ray Trace of the Concentrator with Extended Optics

The design consisted of a fixed collimating lens, two turning mirrors and a focusing lens that could be moved axially

providing 5 inches of movement relative to ground level. Shown in the ray trace are rays that miss the exit lens due to vignetting. The affect on performance of this vignetting was only a few percent and therefore considered acceptible. The exit focusing lens was chosen with a focal length that was shorter than the inlet collimating lens such that the size of the new focal point was reduced by a factor of approximately two. The addition of the lenses and mirrors introduces more power losses but the spot size reduction at the focus would more than make up the power loss by increasing the energy density in the spot.

The mechanical design for holding the lenses and mirrors is shown in Fig. 22. Shown in the figures are three servo motors. The largest provides rotation of the assembly about the central axis of the Cassegrain system. The smaller motor provides tilt on one axis such that by rotation and tilt any points can be achieved within the maximum diameter of the resulting circle. The second motor located on the axial adjustment tube provides axial movement of the focusing lens to account for ground level changes. The present design provides for moving the focal point to a location from 18 inches (45.7 cm) to 23 inches (58.4 cm) from the back of the primary concentrator. Construction of the system was begun as shown in Fig. 23.

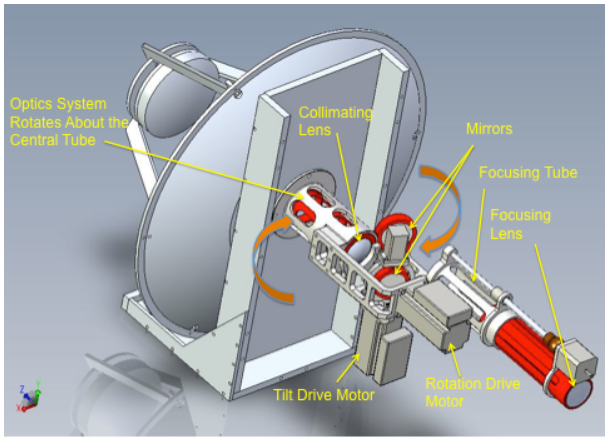

Figure 22. Illustration of Extended Optics Components Attached to the Concentrator

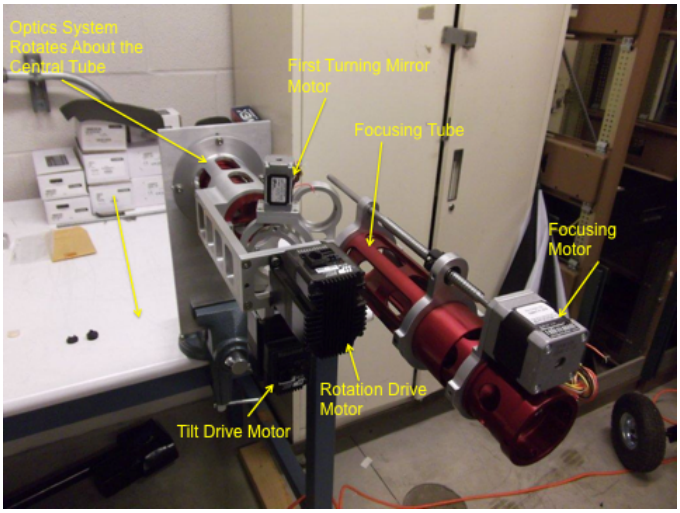

Figure 23. Extended Optics System Buildup

V. Summary

The Cassegrain Concentrator design and test program has produced the following results to date:

1. All required system and test support hardware have been successfully designed and fabricated. The Cassegrain system with regolith tray has been successfully operated. The extended optics system has not yet been added to the Cassegrain system. Software to automatically provide solar tracking and operation of the extended optics system is being developed.

2. A successful silver coating on the primary and secondary concentrators of the Cassegrain system has not been successfully achieved. Power provided to the focal point has been significantly lower than planned. A third try to achieve a silver coating is in process. If this try is not successful the concentrators will be coated with aluminum.

3. All testing to date has provided a melt of the simulated lunar regolith. The melt sizes have been consistent with the power level measured at the focal plane.

4. The last melt test conducted with the thermocouple rake in place yielded a melt with apparent power density much less than previously predicted during ISRU testing. This was determined assuming a Gaussian distribution of the power at the focus. The peak power at the center may be significantly higher than estimated using the Gaussian assumption. An infrared camera with be added in future testing to better understand the power distribution at the focal plane.

5. If the peak power density to produce a melt is proven to be as low as found in the testing other types of concentrators with lower concentration ratios can be considered for lunar use. A Fresnel lens supported by an inflatable torus ring could be considered. This would allow the sunlight to be focused directly through the lens to the ground or to the inlet of an extended optics system and then to the ground.

6. At regolith melt temperature the infrared heat loss to the surroundings from the surface area of the melt is significant. It will always be necessary to minimize the aperture through which the solar beam is applied to the melt to reduce the heat loss during operation.

Even with reduced power the testing to date has provided very good data both in achieving successful melts but also in understanding the operation of the tracking system. The development of test support equipment like the calorimeter and thermocouple rake have been very successful and have provided a tool to better understand the melt process.

VI. References

[1]Gokoglu, S., "Analysis of Thermal and Reaction Times for Hydrogen Reduction of Lunar Regolith", NASA/TM—2009-215623 April 2009

[2]Balasubramaniam, R., Gokoglu, S, and Hegde, U," The Reduction of Lunar Regolith by Carbothermal Processing Using Methane", NASA/TM—2010-216927, November 2010

[3]Balasubramaniam, R., Wegeng, R., Gokoglu, S., Suzuki, N., and Sacksteder, K., "Analysis of Solar-Heated Thermal Wadis to Support Extended-Duration Lunar Exploration," 47th AIAA Aerospace Sciences Meeting, AIAA 2009-1339, January 2009.

[4]Macosko, R.P., Colozza, A. , Castle, C. and Sacksteder K.,"A Solar Concentrator Concept for Providing Direct Solar Energy for Oxygen Production at the Lunar South Pole," AIAA-2010-1167, 48th AIAA Aerospace Sciences Meeting, Orlando, FL, Jan 4-7, 2010.

[5]Street, J.W. Jr., Ray, C., Rickman, D., Scheiman, D.A., "Thermal Properties of Lunar Regolith Simulants," NASA/TM—2010-216348.